 CMC, vol.5, no.1, pp.31-42, 2007

Elastic Torsion Bar with Arbitrary Cross-Section Using the Fredholm Integral Equations

Chein-Shan Liu[1,2]

Abstract: By using a meshless regularized integral equation method (MRIEM), the solution of elastic torsion problem of a uniform bar with arbitrary cross-section is presented by the first kind Fredholm integral equation on an artificial circle, which just encloses the bar's cross-section. The termwise separable property of kernel function allows us to obtain the semi-analytical solutions of conjugate warping function and shear stresses. A criterion is used to select the regularized parameter according to the minimum principle of Laplace equation. Numerical examples show the effectiveness of the new method in providing very accurate numerical solutions as compared with the exact ones.

Keyword: Laplace equation, Elastic torsion, Fredholm integral equation, Lavrentiev regularization, Fourier series, Artificial circle

1 Introduction

The elastic torsion of bar is a classical problem in the theory of elasticity [Timoshenko and Goodier (1961); Little (1973)]. This problem may be formulated either in terms of the Neuman boundary value problem of the Laplace equation for the warping function, the Dirichlet boundary value problem of the Laplace equation for the conjugate warping function, or the Dirichlet boundary value problem of the Poisson equation for the stress function. The second formulation seems a good starting point of the present paper.

Although the exact solutions have been found for some popular bars with simple cross-section shapes like as circle, ellipse, rectangle, triangle, etc., in general, for a given arbitrary shape of the bar the finding of the closed-form functions of its torsion, shear stresses as well as rigidity is not an easy task.

Indeed, the explicit solutions are the exception, and if one were to choose an arbitrary shape of bar in use then the geometric complexity commences and then typically the numerical solutions would be indispensable. The series solutions, different coordinate systems, special functions and complex variables have all been used in the elastic torsion problems.

The most widely used numerical methods are finite difference, finite element and boundary element methods. For a complicated shape of the cross-section by using those methods we usually require a large number of nodes and elements to match the geometrical shape. For the uniform bar with polygon cross-section, there were much advanced methods to treat it as reviewed by Hassenpflug (2003). For the solutions of complicated torsion problems the boundary collocation method was also applied by many people as can be seen in the paper by Kolodziej and Fraska (2005); on the other hand, there also appeared the complex polynomial method and the complex variable boundary element method as advocated by Aleynikov and Stromov (2004).

Various numerical methods for solving the Laplace equation are rapidly developed in the last three decades. Recently, Young, Chen and Lee (2005) have proposed a novel meshless method for solving the Laplace equation in arbitrary plane domain. On the other hand, Liu (2007) has proposed the meshless regularized integral equation method to solve the Laplace problem in arbitrary

[1] Department of Mechanical and Mechatronic Engineering, Taiwan Ocean University, Keelung, Taiwan. E-mail: csliu@mail.ntou.edu.tw

[2] Visiting Professor to Department of Mechanical Engineering,The University of British Columbia. Vancouver, B.C. Canada

plane interior or exterior domain, and Liu (2006) has first applied it to solve the elastic torsion problems.

There were two different boundary integral equation methods for the Laplace equation [Chen and Wu (2006)]. One is the double-layer method and another is the Green's boundary formula. Both of these two methods and some details about the numerical methods of them are described by Jaswon and Symm (1977). Our method is different from that two methods, and the new method is more easy to handle because it is a boundary integral equation on a given artificial circle, instead of those on the contour. Very early, Jaswon and Ponter (1963) have formulated the elastic torsion by using the Green's boundary formula as the first kind Fredholm integral equation for the Dirichlet boundary value problem, and the second kind Fredholm integral equation for the Neumann boundary value problem. Unfortunately, these integral equations possess a logarithmic singularity and the kernel functions are not separable.

To the author's best knowledge, there has no report in the open literature to connect the elastic torsion problem with arbitrary shape into this specially simple type integral equation on a circle with a degenerate kernel. We are going to develop a new approach in this paper, such that we only need to solve a simple second kind Fredholm integral equation to offer an effective resolution of this problem. The new method would provide us a semi-analytical solution, and renders a more compendious numerical implementation to solve the elastic torsion problem in an arbitrary plane domain.

The other parts of the present paper are arranged as follows. In Section 2 we derive the first kind Fredholm intergral equation along a given artificial circle. In Section 3 we consider a direct regularization of the first kind Fredholm intergral equation. Then, we derive a two-point boundary value problem, which helps us to derive a semi-analytical solution of the second kind Fredholm intergral equation in Section 4. In Section 5 we propose by using the conjugate gradient method to solve the normal linear equations system and give a criterion to select the regularized parameter. In Section 6 we use some examples to test the new method, and several contour levels of conjugate warping function and normalized shear stress are plotted. Finally, we give conclusions in Section 7.

2 The first kind Fredholm integral equation

It is known that the torsion of an elastic bar comes to Dirichlet's problem for the Poisson equation

$$\Delta\phi(x,y) = -2, \quad (x,y) \in \Omega, \tag{1}$$

$$\phi(x,y) = 0, \quad (x,y) \in \Gamma, \tag{2}$$

where ϕ is the stress function and Γ is the contour which enclosed the bar's cross-section in a plane domain $\Omega \ni (x,y)$.

If one introduces the conjugate warping function $u(x,y)$ [Little (1973)]:

$$u(x,y) = \phi(x,y) + \frac{1}{2}(x^2+y^2), \tag{3}$$

then one will obtain the following Dirichlet's problem for the Laplace equation

$$\Delta u(x,y) = 0, \quad (x,y) \in \Omega, \tag{4}$$

$$u(x,y) = \frac{x^2+y^2}{2}, \quad (x,y) \in \Gamma. \tag{5}$$

The warping function v together with u constitute an analytic complex function, and they satisfy the Cauchy-Riemann equations:

$$v_x = u_y, \quad v_y = -u_x. \tag{6}$$

If the bar is oriented along the z-direction and assume that the shear modulus is G and β is the twist angle per unit length, then the shear stresses in the cross-section along the x- and y-direction are, respectively,

$$\tau_{xz} = G\beta(u_y - y), \quad \tau_{yz} = -G\beta(u_x - x). \tag{7}$$

It is easy to derive

$$\tau := \frac{\sqrt{\tau_{xz}^2 + \tau_{yz}^2}}{G\beta} = \sqrt{(u_r - r)^2 + u_\theta^2/r^2}, \tag{8}$$

where τ is a normalized shear stress.

In this paper we will propose a new method to solve the problem which consists of the Laplace equation and Cauchy data on a non-circular boundary:

$$\Delta u = u_{rr} + \frac{1}{r}u_r + \frac{1}{r^2}u_{\theta\theta} = 0, \tag{9}$$

$$u(\rho,\theta) = h(\theta),\ \ 0 \le \theta \le 2\pi, \tag{10}$$

where $h(\theta)$ is a given function, and $r = \rho(\theta)$ is a given contour describing the shape of the bar. The contour Γ by using the polar coordinates is given by $\Gamma = \{(r,\theta)|r = \rho(\theta),\ 0 \le \theta \le 2\pi\}$. Here, we do not require to impose any smooth requirement on the shape function $\rho(\theta)$, in addition the continuity.

We replace Eq. (10) by the following boundary condition:

$$u(R_0,\theta) = f(\theta),\ \ 0 \le \theta \le 2\pi, \tag{11}$$

where $f(\theta)$ is an unknown function to be determined, and R_0 is a given positive constant, such that the disk $D = \{(r,\theta)|r \le R_0,\ 0 \le \theta \le 2\pi\}$ can cover the entire domain Ω of the considered problem. Specifically, we may let

$$R_0 = \rho_{\max} = \max_{\theta\in[0,2\pi]} \rho(\theta). \tag{12}$$

Here, the basic idea is to replace the original boundary condition (10) on a complicated contour by a simpler boundary condition (11) on a specified circle, which being much simpler than the given contour. However, the price we should pay is that we require to derive a new equation to solve $f(\theta)$. If this task can be performed and if the function $f(\theta)$ is available, then the advantage of this replacement is that we have a closed-form solution in terms of the Poisson integral:

$$u(r,\theta) = \frac{1}{2\pi}\int_0^{2\pi} \frac{R_0^2 - r^2}{R_0^2 - 2R_0 r\cos(\theta-\xi) + r^2} \cdot f(\xi)d\xi. \tag{13}$$

In the above, R_0 is the radius of an artificial circle, and $f(\theta)$ is an unknown function to be determined on this artificial circle. Because R_0 is uniquely determined by the contour of the considered problem by Eq. (12), we do not worry how to choose a suitable R_0.

By utilizing the technique of separation of variables we are apt to write a Fourier series expansion of $u(r,\theta)$ satisfying Eqs. (9) and (11):

$$u(r,\theta) = a_0 + \sum_{k=1}^{\infty}\left[a_k\left(\frac{r}{R_0}\right)^k \cos k\theta + b_k\left(\frac{r}{R_0}\right)^k \sin k\theta\right], \tag{14}$$

where

$$a_0 = \frac{1}{2\pi}\int_0^{2\pi} f(\xi)d\xi, \tag{15}$$

$$a_k = \frac{1}{\pi}\int_0^{2\pi} f(\xi)\cos k\xi d\xi, \tag{16}$$

$$b_k = \frac{1}{\pi}\int_0^{2\pi} f(\xi)\sin k\xi d\xi. \tag{17}$$

By imposing the condition (10) on Eq. (14) we obtain

$$a_0 + \sum_{k=1}^{\infty}\left[a_k\left(\frac{\rho}{R_0}\right)^k \cos k\theta + b_k\left(\frac{\rho}{R_0}\right)^k \sin k\theta\right] = h(\theta). \tag{18}$$

Substituting Eqs. (15)-(17) into Eq. (18) leads to the first kind Fredholm integral equation:

$$\int_0^{2\pi} K(\theta,\xi)f(\xi)d\xi = h(\theta), \tag{19}$$

where

$$K(\theta,\xi) = \frac{1}{2\pi} + \frac{1}{\pi}\sum_{k=1}^{\infty} B_k[\cos k\theta\cos k\xi + \sin k\theta\sin k\xi] \tag{20}$$

is a kernel function, and

$$B_k(\theta) := \frac{\rho^k(\theta)}{R_0^k}. \tag{21}$$

Up to this point, we have derived an integral equation (19), whose kernel has a special structure of the degenerate type. If the coefficients B_k are constants, from Eq. (19) we can derive a closed-form solution for $f(\theta)$. Regrettably, B_k are not constants and usually they are the functions of θ due to the non-circular nature of the considered problem. Although we have encountered this difficulty, it would be appreciated this type formulation in the below.

3 The second kind Fredholm integral equation

In order to obtain $f(\theta)$ we have to solve the first kind Fredholm integral equation (19). However, this integral equation is known to be ill-posed. We assume that there exists a regularized parameter $\alpha > 0$, such that Eq. (19) can be improved by

$$\alpha f(\theta) + \int_0^{2\pi} K(\theta,\xi) f(\xi) d\xi = h(\theta), \tag{22}$$

which is known as one of the second kind Fredholm integral equation. The above regularization method to obtain a regularized solution by solving the singularly perturbed equation is usually called the Lavrentiev regularization method [Lavrentiev (1967)].

Here, we first prove that the kernel function in Eq. (22) is integrable. By definition (20),

$$|K(\theta,\xi)| \le \frac{1}{2\pi} + \frac{1}{\pi}\sum_{k=1}^{\infty} |\cos k\theta \cos k\xi + \sin k\theta \sin k\xi| \tag{23}$$

can be achieved, because of $\rho \le R_0$ by Eq. (12). For each k, the term $|\cos k\theta \cos k\xi + \sin k\theta \sin k\xi|$ is an integrable function on $[0,2\pi]\times[0,2\pi]$. The linear combination of integrable functions is also an integrable function, due to the linearity of L^2 space; hence, the right-hand side of Eq. (23) is integrable. This implies that $K(\theta,\xi)$ is an integrable function, such that $K(\theta,\xi) \in L^2_{[0,2\pi]\times[0,2\pi]}$. In addition, we suppose that $h(\theta)/\alpha \in L^2_{[0,2\pi]}$ for some $\alpha > 0$. This requirement is always feasible, if the function $h(\theta) \in L^2_{[0,2\pi]}$, which can be satisfied for the most physical applications.

Then, by employing the second Fredholm integral theorem [Mikhlin (1964)], it asserts that Eq. (22) has a unique solution given by

$$f(\theta) = \frac{1}{\alpha} h(\theta) - \int_0^{2\pi} H(\theta,\xi) \frac{1}{\alpha} h(\xi) d\xi, \tag{24}$$

where $H(\theta,\xi)$ is a resolvent kernel.

In general, it is also difficult to find the resolvent kernel function $H(\theta,\xi)$, since $H(\theta,\xi)$ itself must satisfy a resolvent integral equation. We will propose a constructive method to solve Eq. (22) semi-analytically. For this purpose, we assume that the kernel function can be approximated by m terms with

$$K(\theta,\xi) = \frac{1}{2\pi} + \frac{1}{\pi}\sum_{k=1}^{m} B_k \left[\cos k\theta \cos k\xi + \sin k\theta \sin k\xi\right]. \tag{25}$$

This assumption is for the convenience of our derivation, but is not an essential one.

By inspection we have

$$K(\theta,\xi) = \mathbf{P}(\theta)\cdot\mathbf{Q}(\xi), \tag{26}$$

where

$$\mathbf{P}(\theta) := \begin{bmatrix} 1 \\ B_1\cos\theta \\ B_1\sin\theta \\ B_2\cos 2\theta \\ B_2\sin 2\theta \\ \vdots \\ B_m\cos m\theta \\ B_m\sin m\theta \end{bmatrix}, \quad \mathbf{Q}(\xi) := \frac{1}{\pi}\begin{bmatrix} \frac{1}{2} \\ \cos\xi \\ \sin\xi \\ \cos 2\xi \\ \sin 2\xi \\ \vdots \\ \cos m\xi \\ \sin m\xi \end{bmatrix} \tag{27}$$

are $2m+1$-vectors. The dot between $\mathbf{P}$ and $\mathbf{Q}$ denotes the inner product, which is sometimes written as $\mathbf{P}^{\mathrm{T}}\mathbf{Q}$ for convenience, where the superscript T signifies the transpose.

With the aid of Eq. (26), Eq. (22) can be decomposed as

$$\alpha f(\theta) + \int_0^{\theta} \mathbf{P}^{\mathrm{T}}(\theta)\mathbf{Q}(\xi) f(\xi) d\xi + \int_{\theta}^{2\pi} \mathbf{P}^{\mathrm{T}}(\theta)\mathbf{Q}(\xi) f(\xi) d\xi = h(\theta). \tag{28}$$

Let us define

$$\mathbf{u}_1(\theta) := \int_0^{\theta} f(\xi)\mathbf{Q}(\xi) d\xi, \tag{29}$$

$$\mathbf{u}_2(\theta) := \int_{2\pi}^{\theta} f(\xi)\mathbf{Q}(\xi) d\xi, \tag{30}$$

and then Eq. (28) can be expressed as

$$\alpha f(\theta) + \mathbf{P}^{\mathrm{T}}(\theta)[\mathbf{u}_1(\theta) - \mathbf{u}_2(\theta)] = h(\theta). \tag{31}$$

Taking the differentials of both Eqs. (29) and (30) with respect to θ, we obtain

$$\mathbf{u}_1'(\theta) = \mathbf{Q}(\theta) f(\theta), \tag{32}$$

$$\mathbf{u}_2'(\theta) = \mathbf{Q}(\theta) f(\theta). \tag{33}$$

Inserting Eq. (31) for $f(\theta)$ into the above two equations we obtain

$$\alpha \mathbf{u}_1'(\theta) = \mathbf{Q}(\theta)\mathbf{P}^{\mathrm{T}}(\theta)[\mathbf{u}_2(\theta) - \mathbf{u}_1(\theta)] + h(\theta)\mathbf{Q}(\theta), \tag{34}$$

$$\alpha \mathbf{u}_2'(\theta) = \mathbf{Q}(\theta)\mathbf{P}^{\mathrm{T}}(\theta)[\mathbf{u}_2(\theta) - \mathbf{u}_1(\theta)] + h(\theta)\mathbf{Q}(\theta), \tag{35}$$

$$\mathbf{u}_1(0) = \mathbf{0}, \quad \mathbf{u}_2(2\pi) = \mathbf{0}, \tag{36}$$

where the last two conditions follow from Eqs. (29) and (30) immediately. The above equations constitute a two-point boundary value problem.

4 Semi-analytical solution

In this section we will find a semi-analytical solution of $f(\theta)$. From Eqs. (32) and (33) it can be seen that $\mathbf{u}_1' = \mathbf{u}_2'$, which means that

$$\mathbf{u}_1 = \mathbf{u}_2 + \mathbf{c}, \tag{37}$$

where $\mathbf{c}$ is a constant vector to be determined. By using the second condition in Eq. (36) we find that

$$\mathbf{u}_1(2\pi) = \mathbf{u}_2(2\pi) + \mathbf{c} = \mathbf{c}. \tag{38}$$

From Eqs. (29) and (38) it follows that

$$\mathbf{c} = \int_0^{2\pi} f(\xi)\mathbf{Q}(\xi)d\xi, \tag{39}$$

whose mathematical meaning is that $\mathbf{c}$ is a vector of the Fourier coefficients of the unknown function $f(\theta)$.

Substituting Eq. (37) into (34) we have

$$\alpha \mathbf{u}_1'(\theta) = h(\theta)\mathbf{Q}(\theta) - \mathbf{Q}(\theta)\mathbf{P}^{\mathrm{T}}(\theta)\mathbf{c}. \tag{40}$$

Integrating the above equation and using the first condition in Eq. (36) it follows that

$$\alpha \mathbf{u}_1(\theta) = \int_0^{\theta} h(\xi)\mathbf{Q}(\xi)d\xi - \int_0^{\theta} \mathbf{Q}(\xi)\mathbf{P}^{\mathrm{T}}(\xi)d\xi\mathbf{c}. \tag{41}$$

Taking $\theta = 2\pi$ in the above equation and imposing the condition (38), we obtain a governing equation for $\mathbf{c}$:

$$\mathbf{R}\mathbf{c} = \int_0^{2\pi} h(\xi)\mathbf{Q}(\xi)d\xi, \tag{42}$$

where

$$\mathbf{R} := \alpha \mathbf{I}_{2m+1} + \int_0^{2\pi} \mathbf{Q}(\xi)\mathbf{P}^{\mathrm{T}}(\xi)d\xi \tag{43}$$

is a constant $(2m+1)\times(2m+1)$ matrix.

By Eqs. (39) and (42) we have

$$\int_0^{2\pi} f(\xi)\mathbf{Q}(\xi)d\xi = \mathbf{R}^{-1}\int_0^{2\pi} h(\xi)\mathbf{Q}(\xi)d\xi, \tag{44}$$

which describes the relation between the Fourier coefficients of two boundary functions $f(\theta)$ and $h(\theta)$.

On the other hand, from Eqs. (31) and (37) we have

$$\alpha f(\theta) = h(\theta) - \mathbf{c}\cdot\mathbf{P}(\theta). \tag{45}$$

For each selected α, after obtaining $\mathbf{c}$ by numerical method, we can use Eq. (45) to calculate the boundary function $f(\theta)$ along an artificial circle with radius R_0, from which we can insert any specified (r,θ) into the series solution (14) up to $k = m$ to calculate $u(r,\theta)$.

By inserting

$$u_r = \sum_{k=1}^{m}\left(k a_k \frac{r^{k-1}}{R_0^k}\cos k\theta + k b_k \frac{r^{k-1}}{R_0^k}\sin k\theta\right), \tag{46}$$

$$\frac{u_\theta}{r} = \sum_{k=1}^{m}\left(k b_k \frac{r^{k-1}}{R_0^k}\cos k\theta - k a_k \frac{r^{k-1}}{R_0^k}\sin k\theta\right) \tag{47}$$

into Eq. (8) we can calculate the normalized shear stress. It can be seen that the present approach has a great advantage to derive the semi-analytical solutions of both the conjugate warping function and shear stresses.

From Eq. (42), it is straightforward to write

$$\mathbf{c} = \mathbf{R}^{-1} \int_0^{2\pi} h(\xi)\mathbf{Q}(\xi)d\xi. \tag{48}$$

Inserting the above equation into Eq. (45) we obtain

$$f(\theta) = \frac{1}{\alpha}h(\theta) - \int_0^{2\pi} \mathbf{P}(\theta)\cdot\mathbf{R}^{-1}\mathbf{Q}(\xi)\frac{1}{\alpha}h(\xi)d\xi. \tag{49}$$

Upon viewing $\mathbf{P}(\theta)\cdot\mathbf{R}^{-1}\mathbf{Q}(\xi)$ as an approximation of the resolvent kernel $H(\theta,\xi)$, we indeed provide a numerical solution of Eq. (22) as specified in Section 3.

In summary, the present method used a regularized integral equation to solve the boundary function $f(\theta)$ along an artificial circle, which just enclosed the bar's cross-section. Then, by using the Fourier series solutions to obtain the potential function and shear stresses. In this sense, we call the new method a *meshless regularized integral equation method* (MRIEM).

5 The conjugate gradient method

Given the boundary function $h(\theta)$, the right-hand side of Eq. (42) can be evaluated by, for example, a trapezoidal quadrature. Hence, from Eq. (42) we obtain a linear equations system with $\mathbf{R}$ calculated by Eq. (43). The $\mathbf{R}$ may be not a positive definite matrix. Therefore, instead of Eq. (42) we consider the normal equation:

$$\mathbf{A}\mathbf{c} = \mathbf{b}, \tag{50}$$

where

$$\mathbf{A} := \mathbf{R}^{\mathrm{T}}\mathbf{R}, \tag{51}$$

$$\mathbf{b} = \mathbf{R}^{\mathrm{T}} \int_0^{2\pi} h(\xi)\mathbf{Q}(\xi)d\xi. \tag{52}$$

Eq. (50) is better than Eq. (42), since $\mathbf{A}$ is positive definite.

An effective method to solve linear equations is the conjugate gradient method, which enhances the searching direction of minimum by imposing the orthogonality of the residual vectors at each different iterative step [Jacoby, Kowalik and Pizzo (1972)]. The algorithm of conjugate gradient method can be summarized as follows:

(i) Give an initial $\mathbf{c}_0$.

(ii) Calculate $\mathbf{r}_0 = \mathbf{b} - \mathbf{A}\mathbf{c}_0$ and $\mathbf{p}_1 = \mathbf{r}_0$.

(iii) For $k = 1, 2\ldots$ we repeat the following calculations:

$$\eta_k = \frac{\|\mathbf{r}_{k-1}\|^2}{\mathbf{p}_k^{\mathrm{T}}\mathbf{A}\mathbf{p}_k}, \tag{53}$$

$$\mathbf{c}_k = \mathbf{c}_{k-1} + \eta_k\mathbf{p}_k, \tag{54}$$

$$\mathbf{r}_k = \mathbf{r}_{k-1} - \eta_k\mathbf{A}\mathbf{p}_k, \tag{55}$$

$$r_k = \frac{\|\mathbf{r}_k\|^2}{\|\mathbf{r}_{k-1}\|^2}, \tag{56}$$

$$\mathbf{p}_{k+1} = \mathbf{p}_k + r_k\mathbf{p}_k. \tag{57}$$

If $\mathbf{c}_k$ converges according to a given stopping criterion:

$$\|\mathbf{c}_{k+1} - \mathbf{c}_k\| < \varepsilon, \tag{58}$$

then stop; otherwise, go to step (iii).

It is known that for the Laplace equation the maximum and minimum of u are occurred on the boundary. This point can be employed to derive an efficient criterion to select a suitable regularized parameter α. Let

$$\rho_{\min} = \min_{\theta\in[0,2\pi]} \rho(\theta). \tag{59}$$

Then, for each given boundary $\rho(\theta)$ the minimum of u along the contour is given by the boundary data in Eq. (5) with

$$u_{\min} = \frac{1}{2}\rho_{\min}^2. \tag{60}$$

When we insert the value $r = \rho_{\min}$ in the numerical solution, we obtain $u(\rho_{\min},\theta)$, of which we require that the minimum of $u(\rho_{\min},\theta)$ obtained from the numerical solution is coincident with the one in Eq. (60); otherwise, we may adjust the regularized parameter α until the correct minimum is obtained.

Table 1: Comparison of exact and numerical solutions of u

x	y	u-exact	$\hat{u}$-CBEM	$\lvert\varepsilon_u\rvert(\%)$ CBEM	$\hat{u}$-PIES	$\lvert\varepsilon_u\rvert(\%)$PIES	$\hat{u}$-MRIEM	$\lvert\varepsilon_u\rvert(\%)$ MRIEM
-0.5	0.0	0.645833	0.6557	1.53	0.64585	0.00310	0.645833	0
0.0	0.0	0.666667	0.6763	1.44	0.66668	0.00150	0.666664	0.00045
0.5	0.0	0.687500	0.6969	1.37	0.68751	0.00145	0.687493	0.00102
1.0	0.0	0.833333	0.8417	1.01	0.83336	0.00360	0.833318	0.00180
1.5	0.0	1.229167	1.2302	0.08	1.22809	0.08786	1.229137	0.00244
-0.5	0.5	0.708333	0.7180	1.36	0.70833	0	0.708332	0.00014
0.0	0.5	0.666667	0.6763	1.44	0.66668	0.00300	0.666665	0.00030
0.5	0.5	0.625000	0.6347	1.55	0.62443	0.09120	0.624998	0.00032
-0.5	1.0	0.895833	0.9046	0.98	0.89594	0.01228	0.895830	0.00033

Table 2: Comparison of exact and numerical solutions of τ

x	y	τ-exact	$\hat{\tau}$-BEM	$\lvert\varepsilon_\tau\rvert(\%)$ BEM	$\hat{\tau}$-CVBEM	$\lvert\varepsilon_\tau\rvert(\%)$ CVBEM	$\hat{\tau}$-MRIEM	$\lvert\varepsilon_\tau\rvert(\%)$ MRIEM
$-\sqrt{3}/3$	0.0	0.8660	0.869	0.346	0.953	10	0.8657	0.035
$-\sqrt{3}/3$	0.15	0.8465	0.847	0.059	0.842	0.532	0.8464	0.012
$-\sqrt{3}/3$	0.325	0.7746	0.775	0.052	0.763	1.498	0.7746	0
$-\sqrt{3}/3$	0.525	0.6273	0.630	0.43	0.621	1.004	0.6273	0
$-\sqrt{3}/3$	0.75	0.3789	0.380	0.284	0.404	6.624	0.3790	0.026

6 Numerical examples

6.1 An elliptical cross-section

At first let us consider the torsion of a bar whose cross-section is an ellipse with semiaxes a and b, and the contour in the polar coordinates is described by

$$\rho(\theta)=\frac{ab}{\sqrt{a^2\sin^2\theta+b^2\cos^2\theta}}. \tag{61}$$

For this case we have a boundary condition

$$u(\rho,\theta)=h(\theta)=\frac{a^2b^2}{2(a^2\sin^2\theta+b^2\cos^2\theta)}. \tag{62}$$

The exact solution of u is known to be [Timoshenko and Goodier (1961)]

$$u(r,\theta)=\frac{a^2b^2}{a^2+b^2}+\frac{a^2-b^2}{2(a^2+b^2)}r^2\cos 2\theta. \tag{63}$$

We have applied the numerical method MRIEM on this example. The parameters used in this calculation are $m=10$, $a=2$, $b=1$, and $\alpha=2.1\times10^{-6}$, and only nine iterations are used to calculate $\mathbf{c}$, which starting from an initial $\mathbf{c}=\mathbf{0}$ under a stopping criterion with $\varepsilon=10^{-8}$.

In Fig. 1(a) the numerical result of $u(r,\theta)$ at $r=1$ is compared with the exact one, which is obtained from Eq. (63) by inserting $r=1$. The numerical error as shown in Fig. 1(b) can be seen in the order of 10^{-6} and the numerical solution is very accurate. The major part of the numerical error is due to the numerical integrations of Eqs. (15)-(17), of which we have used 150 subintervals in the trapezoidal quadratures.

6.2 An equilateral triangle cross-section

Let us consider the torsion of a bar whose cross-section is an equilateral triangle with length a of the vertical line as shown in Fig. 2(a). The contour in the polar coordinates can be described by

$$\rho(\theta)=\begin{cases}\dfrac{a}{3\sin(\theta+\pi/6)} & 0\le\theta<\frac{2\pi}{3},\\ \dfrac{-a}{3\cos\theta} & \frac{2\pi}{3}\le\theta<\frac{4\pi}{3},\\ \dfrac{-a}{3\sin(\theta-\pi/6)} & \frac{4\pi}{3}\le\theta<2\pi.\end{cases} \tag{64}$$

The exact solutions are known to be [Hromadka

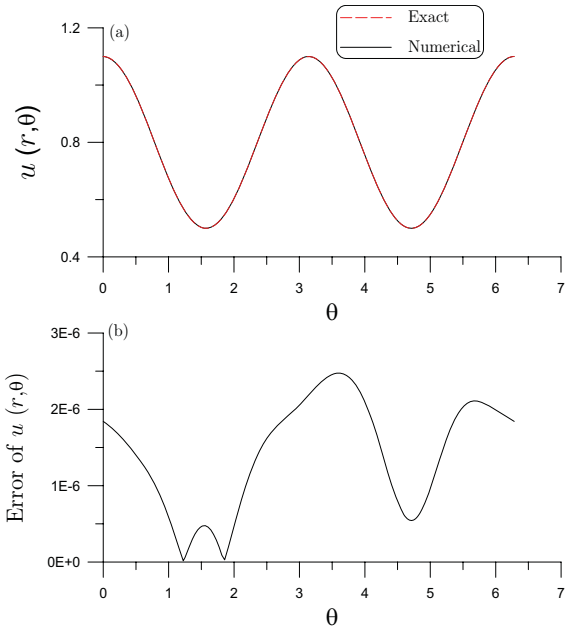

Figure 1: For an elliptical bar (a) comparing numerical solution with exact solution, and (b) plotting the numerical error.

and Lai (1987)]

$$u(x,y) = \frac{1}{2a}(x^3 - 3xy^2) + \frac{2a^2}{27}, \tag{65}$$

$$\tau_{xz} = -G\beta\left(y + \frac{3xy}{a}\right), \tag{66}$$

$$\tau_{yz} = G\beta\left(x + \frac{3y^2 - 3x^2}{2a}\right). \tag{67}$$

In Table 1 we present the exact solutions computed from Eq. (65) at several different points and the approximated results obtained by a well-known method–CBEM [Hromadka and Lai (1987)], the results obtained by Zieniuk (2003) with the parametric integral equation system (PIES), and also by our numerical method–MRIEM, of which $a = 3$, $m = 15$, $\alpha = 1.03 \times 10^{-5}$ and the stopping criterion with $\varepsilon = 10^{-8}$ were used in the calculations. Table 1 also includes the relative errors $|\varepsilon_u| = |(u - \hat{u})/u|$. It is evident that the numerical method MRIEM can calculate the functions $\hat{u}$, which are much accurate than that of the CBEM and are also better than the PIES. We also plotted the contour curves of the normalized shear stress in Fig. 2(a). They

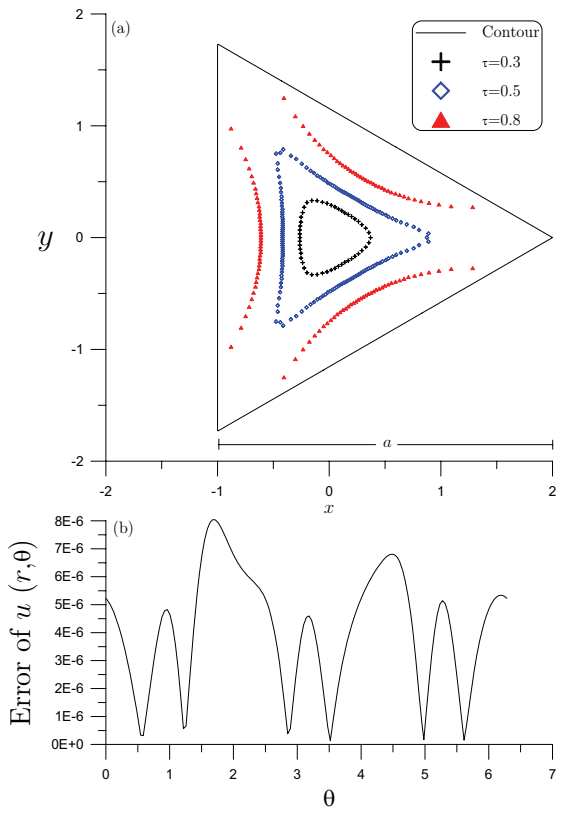

Figure 2: For an equilateral triangular bar with $a = 3$ the contour levels of shear stress were plotted in (a), and (b) plotting the numerical error.

are almost coincident with the exact results calculated from Eqs. (66) and (67).

In Fig. 2(b) the numerical result of $u(r,\theta)$ at $r = 1$ is compared with the exact one, which is obtained from Eq. (65) by inserting $x = \cos\theta$ and $y = \sin\theta$. The numerical error as shown in Fig. 2(b) is in the order of 10^{-6} and the numerical solution is very accurate.

Now, we turn our attention to the comparisons of the normalized shear stress defined by Eq. (8). At several points at the bottom of the triangular with $a = \sqrt{3}$, the exact solutions of shear stress are obtained by substituting Eqs. (66) and (67) and inserting the different (x,y) as shown in Table 2 into Eq. (8). The solutions with CVBEM and with BEM are obtained by Aleynikov and Stromov (2004). Our results marked by MRIEM are calculated by inserting Eqs. (46) and (47) into Eq. (8), where we use $m = 25$ and $\alpha = 1.1 \times 10^{-4}$. Table 2

also includes the relative errors $|\varepsilon_\tau| = |(\tau - \hat{\tau})/\tau|$. It can be seen that the numerical solutions with MRIEM are much better than the other two methods.

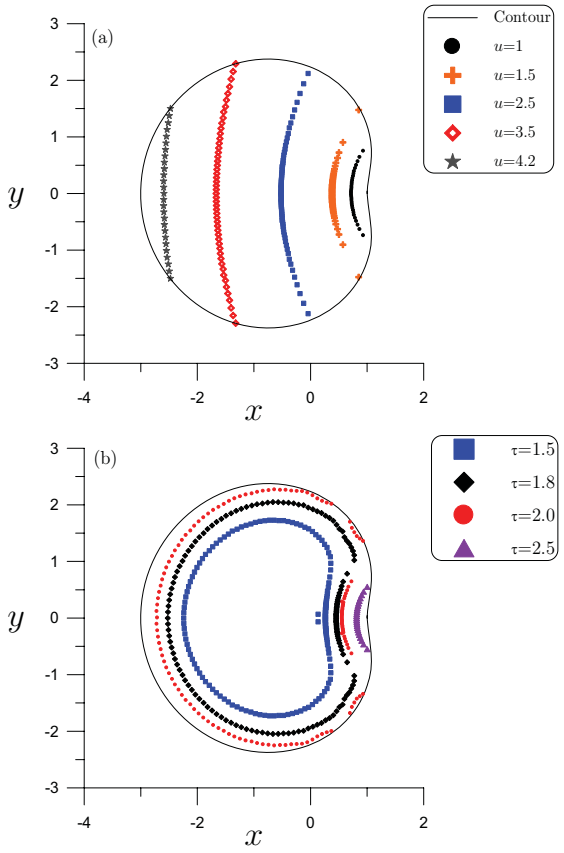

Figure 3: For an epitrochoid bar with $a = 1$ and $b = 1$ the contour levels of conjugate warping function were plotted in (a), and the contour levels of shear stress were plotted in (b).

6.3 *The epitrochoid-shape bars*

Let us consider a more complex torsion problem of the epitrochoid-shape bar described by

$$\rho(\theta) = \sqrt{(a+b)^2 + 1 - 2(a+b)\cos(a\theta/b)}, \tag{68}$$

$$x(\theta) = \rho\cos\theta, \quad y(\theta) = \rho\sin\theta, \tag{69}$$

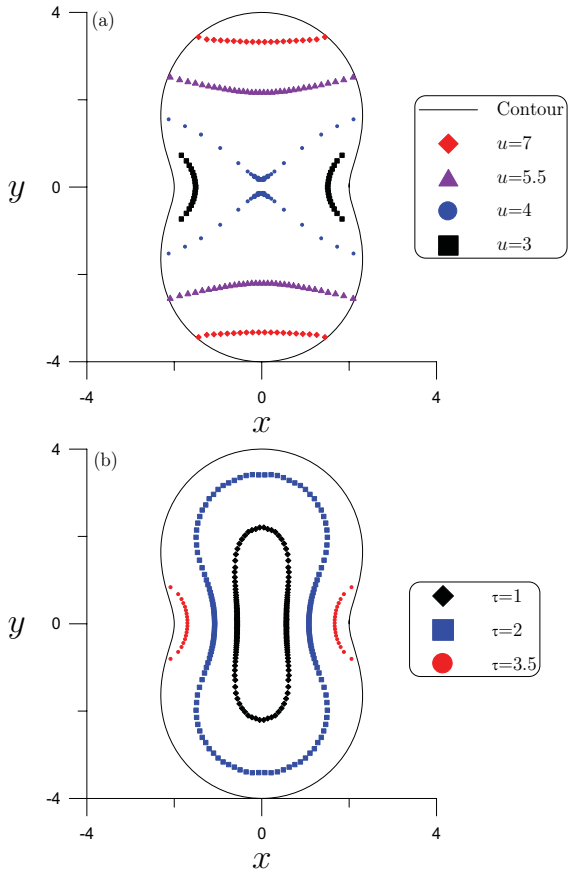

Figure 4: For an epitrochoid bar with $a = 2$ and $b = 1$ the contour levels of conjugate warping function were plotted in (a), and the contour levels of shear stress were plotted in (b).

which is equipped with a boundary condition

$$u(\rho,\theta) = h(\theta) = \frac{1}{2}[(a+b)^2 + 1 - 2(a+b)\cos(a\theta/b)]. \tag{70}$$

For this problem we have no closed-form solution. Let $a = 1,2,3$ and $b = 1$ we can apply the MRIEM on this problem. For $a = 1, b = 1$, the parameters used are $m = 25$ and $\alpha = 0.0025$. For $a = 2,3$ and $b = 1$, the parameters used are $m = 25$ and $\alpha = 0.002$. In all these calculations the stopping criterion with $\varepsilon = 10^{-4}$ was used.

For each case the contour levels of u and normalized shear stress τ are plotted sequentially in Figs. 3-5. The values of u plotted are between the theoretical minimum and maximum given by

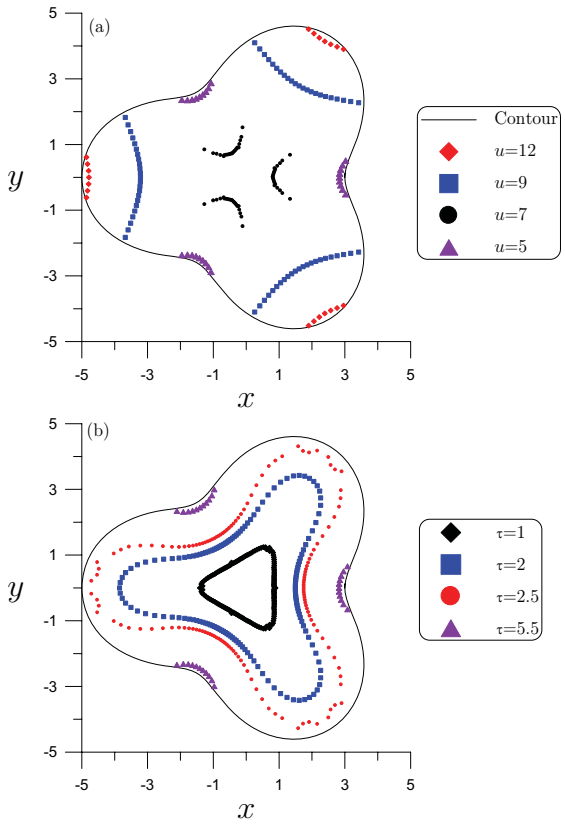

Figure 5: For an epitrochoid bar with $a = 3$ and $b = 1$ the contour levels of conjugate warping function were plotted in (a), and the contour levels of shear stress were plotted in (b).

$u_{\min} = \rho_{\min}^2/2$ and $u_{\max} = \rho_{\max}^2/2$.

6.4 A kite-shaped bar

Then, let us consider the torsion of a bar whose cross-section is a kite-shape described by

$$\rho(\theta) = \sqrt{(0.6\cos\theta + 0.3\cos 2\theta - 0.2)^2 + 0.36\sin^2\theta}, \tag{71}$$

$$x(\theta) = \rho\cos\theta, \quad y(\theta) = \rho\sin\theta. \tag{72}$$

For this case we have a boundary condition

$$u(\rho,\theta) = h(\theta) = \frac{1}{2}[(0.6\cos\theta + 0.3\cos 2\theta - 0.2)^2 + 0.36\sin^2\theta]. \tag{73}$$

By applying the MRIEM on this problem with $m = 25$ and $\alpha = 0.0025$, we have plotted the contour levels of u and τ in Fig. 6(a) for $u = 1.4, 1.8, 2.2, 2.6, 3.0$, and in Fig. 6(b) for $\tau = 0.5, 1, 2, 2.5$.

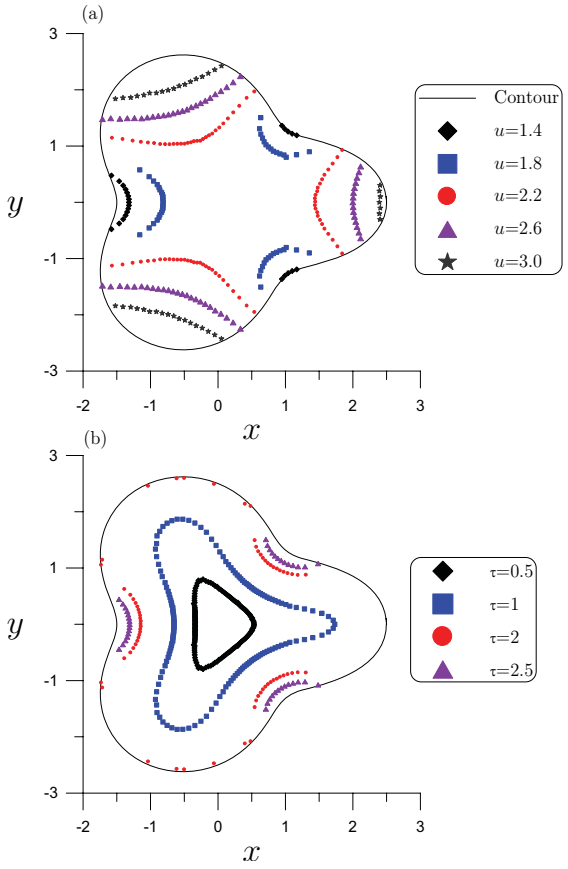

Figure 6: For a kite shaped bar the contour levels of conjugate warping function were plotted in (a), and the contour levels of shear stress were plotted in (b).

6.5 A hypotrochoid bar

Finally, let us consider a hypotrochoid bar described by

$$\rho(\theta) = \sqrt{(a-b)^2 + c^2 + 2(a-b)c\cos(a\theta/b)}, \tag{74}$$

$$x(\theta) = \rho\cos\theta, \quad y(\theta) = \rho\sin\theta. \tag{75}$$

We have applied the MRIEM on this example with $a = 4$, $b = 1$ and $c = 0.5$, whose contour is

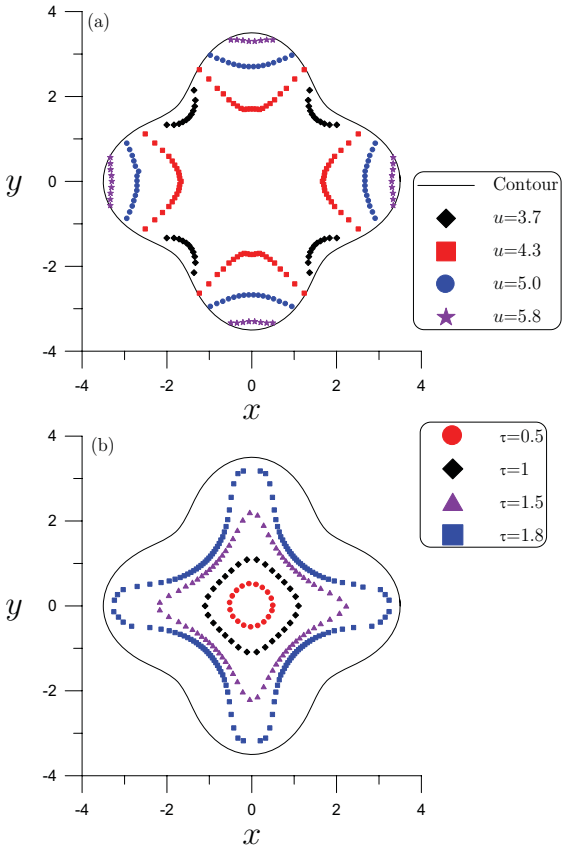

Figure 7: For a hypotrochoid bar with $a = 4, b = 1$ and $c = 0.5$ the contour levels of conjugate warping function were plotted in (a), and the contour levels of shear stress were plotted in (b).

shown in Fig. 7. Under $m = 30$ and $\alpha = 0.0027$, the numerical results of the contour levels of u and τ are plotted in Fig. 7(a) for $u = 3.7, 4.3, 5.0, 5.8$, and in Fig. 7(b) for $\tau = 0.5, 1, 1.5, 1.8$.

7 Conclusions

In this paper we have proposed a new method of MRIEM to calculate the solutions of Laplace equation in the arbitrary plane domains; especially, it is very useful for the elastic torsion problems with complicated shapes of the cross-section. It was demonstrated that only a few Fourier terms is required in the calculations; for most examples, $m = 30$ is enough. In the regularized sense, we could find a semi-analytical solution of the boundary function on an artificial circle, and thus by the Fourier series expansion we can calculate the conjugate warping function and shear stress at any point inside the domain of the considered problem. The conjugate gradient method together with a suitable criterion to pick up the regularized parameter was used to quickly calculate the unknown boundary function on an artificial circle. The numerical examples show that the effectiveness of the new method and the accuracy is very good by comparing with the exact solutions.

References

Aleynikov, S.M.; Stromov, A.V. (2004): Comparison of complex methods for numerical solutions of boundary problems of the Laplace equation. *Eng. Anal. Boundary Elem.*, vol. 28, pp. 615-622.

Chen, J.T.; Wu, C.S. (2006): Alternative derivations for the Poisson integral formula. *Int. J. Math. Educ. Sci. Tech.*, vol. 37, pp. 165-185.

Hassenpflug, W.C. (2003): Torsion of uniform bars with polygon cross-section. *Comp. Math. Appl.*, vol. 46, pp. 313-392.

Hromadka II, T.V.; Lai, C. (1987): The Complex Variable Boundary Element Method in Engineering Analysis. Springer-Verlag, New York.

Jacoby, S.L.S.; Kowalik, J.S.; Pizzo, J.T. (1972): Iterative Methods for Nonlinear Optimization Problems. Prentice-Hall, New Jersey.

Jaswon, M.A.; Ponter, A.R. (1963): An integral equation solution of the torsion problem. *Proc. Roy. Soc. London A*, vol. 273, pp. 237-246.

Jaswon, M.A.; Symm, G.T. (1977): Integral Equation Methods in Potential Theory and Elastostatics. Academic, New York.

Kolodziej, J.A.; Fraska, A. (2005): Elastic torsion of bars possessing regular polygon in cross-section using BCM. *Comp. Struct.*, vol. 84, pp. 78-91.

Lavrentiev, M.M. (1967): Some Improperly Posed Problems of Mathematical Physics. Springer, New York.

Little, R.W. (1973): Elasticity. Prentice-Hall, New Jersey.

Liu, C.-S. (2006): New methods for elastic torsion of bar with arbitrary shape of cross-section. Proceedings of Symposium on Advances of Mechanics. In Honor of President Robert R. Hwang, Keelung, Taiwan, pp. 95-103.

Liu, C.-S. (2007): A meshless regularized integral equation method (MRIEM) for Laplace equation in arbitrary interior or exterior plane domains. Proceedings of ICCES'07, Miami, American, pp. 69-80.

Mikhlin, S.G. (1964): Integral Equations and Their Application. Pergamon Press, New York.

Timoshenko, S.P.; Goodier, J.M. (1961): Theory of Elasticity. McGraw-Hill, New York.

Young, D.L.; Chen, K.H.; Lee, C.W. (2005): Novel meshless method for solving the potential problems with arbitrary domain. *J. Comp. Phys.*, vol. 209, pp. 290-321.

Zieniuk, E. (2003): Bézier curves in the modification of boundary integral equations (BIE) for potential boundary-values problems. *Int. J. Solids Struct.*, vol. 40, pp. 2301-2320.